J Mammal Evol (2012) 19:9–25
DOI 10.1007/s10914-011-9179-5

ORIGINAL PAPER

# An Approach to the Biomechanics of the Masticatory Apparatus of Early Miocene (Santacrucian Age) South American Ungulates (Astrapotheria, Litopterna, and Notoungulata): Moment Arm Estimation Based on 3D Landmarks

**Guillermo H. Cassini · Sergio F. Vizcaíno**

**Abstract** Notoungulates, litopterns, and astrapotheres are among the most representative mammals of the early Miocene Santacrucian Age. They comprise a diversity of biological types and sizes, from small forms, comparable to rodents, to giants with no analogues in modern faunas. Traditionally, all of them have been considered herbivores; this diversity is reflected in different morphologies of the masticatory apparatus, suggesting a variety of feeding habits. The application of biomechanics to the study of fossil mammals is a good approach to test functional hypotheses. Jaws act as a lever system, with the pivot at the temporomandibular joint, with masticatory muscles providing the input force, whereas the output force is produced by the teeth on food. The moment arms of the lines of action of the muscles can be estimated to analyze relationships between bite force and bite velocity. A morphogeometric approach inspired by Vizcaíno et al. (1998) is applied to estimate muscle moment arms in a static 3D bite model based on three-dimensional landmarks and semilandmarks on crania with mandibles in occlusion. This new 3D geometric method to evaluate jaw mechanics demonstrated its reliability when applied to a control sample of extant mammals that included carnivores, herbivores, and omnivores. Our results indicate that, except for *Pachyrukhos*, in no Santacrucian ungulate does the masseter muscle have greater mechanical advantage than the temporalis. Among them, notoungulates have a better configuration to develop force on the molar tooth row than litopterns. This indicates a diet richer in tough plant materials for Santacrucian notoungulates (e.g., grass or even bark) than for litopterns (e.g., dicots). This is consistent with recent ecomorphological approaches applied to this fauna. Finally, the approach proposed here proves to be useful for comparing masticatory performance and it is a powerful tool to validate ecomorphological dietary hypotheses in fossil taxa.

**Keywords** Fossil ungulates · Jaw Biomechanics · Patagonia · Proterotheriidae · Nesodontinae · Typotheria

## Introduction

Several extinct South American native ungulate lineages evolved within the geographical context of isolation during most of the Cenozoic (Bond 1986). They were part of the “first faunal stratum” of Simpson (1950), composed of some endemic families of Condylarthra and the orders Astrapotheria, Litopterna, Notoungulata, Pyrotheria, and Xenungulata (Patterson and Pascual 1968; Simpson 1980; Bond et al. 1995). Although they were all once considered to be united in a single taxon, Meridiungulata, originally founded on the idea that all endemic South American

---

**Electronic supplementary material** The online version of this article (doi:10.1007/s10914-011-9179-5) contains supplementary material, which is available to authorized users.

G. H. Cassini (✉)
División Mastozoología, CONICET,
Museo Argentino de Ciencias Naturales “Bernardino Rivadavia”
Av. Angel Gallardo 470,
C1405DJR, Ciudad Autónoma de Buenos Aires, Argentina
e-mail: gcassini@macn.gov.ar

G. H. Cassini
Departamento de Ciencias Básicas,
Universidad Nacional de Luján,
Buenos Aires, Argentina

S. F. Vizcaíno
División Paleontología de Vertebrados, CONICET,
Museo de La Plata Paseo del Bosque s/n,
B1900FWA, La Plata, Buenos Aires, Argentina
e-mail: vizcaino@fcnym.unlp.edu.ar

ungulates were monophyletic (McKenna 1975), the phylogenetic relationships of these groups are unclear (Cifelli 1985, 1993; Gelfo et al. 2008; Billet 2010). Notoungulates, litopterns, and astrapotheres (Fig. 1) are among the most representative mammals of the early Miocene Santacrucian Age.

Notoungulata constitutes the most abundant and diverse clade of endemic South American ungulates, both taxonomically and morphologically (Simpson 1936; Patterson and Pascual 1972; Cifelli 1993; Croft 1999). Following Billet (2010), the clade comprises two main monophyletic groups, Toxodontia and Typotheria, plus some basal notoungulate families. Toxodonts (Fig. 1a–b) include large to very large animals (i.e., above 44 kg, sensu Martin and Steadman 1999; see Appendix 1) and are sometimes compared to hippos or rhinos, due to their inferred general appearance and to the presence of molar crown patterns suggestive of grinding (Ameghino 1907; Scott 1912; Bond 1999). Typotheres (Fig. 1c–f) are small to medium-sized mammals (see Appendix 1), mostly described as rodent-like in overall form, although different families resemble living wombats (Mesotheriidae), hares (Hegetotheriidae), and hyraxes (Interatheriidae) (Ameghino 1889; Sinclair 1909; Croft 1999; Reguero et al. 2007; Shockey et al. 2007). In both toxodonts and typotheres, there is an apparent tendency to evolve from a generalized masticatory apparatus with complete dentition, with brachydont cheek teeth, and without diastema, to very specialized forms that possess, for instance, hypertrophied incisors, simplified crown patterns, and ever-growing (euhypsodonty sensu Mones 1982) cheek teeth (Ameghino 1887, 1894; Sinclair 1909; Simpson 1967; Cifelli 1985).

After notoungulates, litopterns are the most diverse and abundant clade of endemic South American ungulates (Pascual et al. 1996). They are recorded throughout the Cenozoic, from the early Paleocene (Bonaparte and Morales 1997) to the late Pleistocene (Bondesio 1986; Bond 1999), reaching their greatest taxonomic richness (at the genus level) during the late Miocene, and gradually diminishing throughout the Pliocene with forms that become progressively more specialized, until their extinction by the late Pleistocene-early Holocene (see Bond et al. 1995). Following Cifelli (1993) and Muizon and Cifelli (2000), the clade is monophyletic, though Billet's (2010) analysis does not support its monophyly. The two families most represented are Macraucheniidae and Proterotheriidae. Macraucheniids (Fig. 1g) include large to very large animals (see Appendix 1), with an inferred general appearance resembling living camels or llamas (Scott 1913; Bond 1999). Proterotheriids (Fig. 1h–k) are medium-sized to large-sized mammals (see Appendix 1) mostly described as similar to primitive holarctic horses due to the convergent presence of reduced digits and mesaxonic limbs (Ameghino 1898), although their tooth crown morphology resembles that of artiodactyls like deer and camels (Bond et al. 2001).

The third clade, astrapotheres, is less diverse and abundant than the two above mentioned. However, they constitute a very peculiar order of native ungulates from the Tertiary of South America. They are recorded from the Paleocene (Soria and Powell 1981) to the middle Miocene (Johnson and Madden 1997). They attained their maximum taxonomic richness during the early Miocene Colhuehuapian and Santacrucian ages (see below and Marshall and Cifelli 1989; Johnson and Madden 1997). According to Cifelli (1993), Astrapotheria are a monophyletic clade and, following Billet (2010), they constitute the sister group of Notoungulata. In the coastal exposures of the Santa Cruz Formation (Santacrucian Age), they are represented by a single genus, *Astrapotherium* Burmeister, 1879 (Fig. 1l), which together with *Astrapothericulus* Ameghino, 1902, constitute the most derived taxa (Astrapotheriinae) among astrapotheres (Kramarz 2009). *Astrapotherium* species are large to very large mammals (including strict megamammals, i.e., 1000 kg or more, sensu Owen-Smith 1988; see Appendix 1). They are described as morphologically intermediate between a tapir and an elephant, characterized by their large canine tusks, brachydont cheek teeth, loss of all upper incisors and some premolars, and nasal retraction that suggest a putative tapir-like proboscis (Scott 1913, 1928; Riggs 1935; Kramarz 2009). Since Scott (1913), astrapotheres have been considered inhabitants of riparian or meadow habitats, thought to have fed upon lush vegetation (Riggs 1935; Scott 1937). Furthermore, they are considered good indicators of lowland continental environments (Marshall et al. 1990). Based on enamel structure, Rensberger and Pfretzschner (1992) concluded that astrapothere cheek teeth had similar function and mechanical demands to the teeth of extant rhinoceroses.

As described below, the early Miocene ungulates comprise a diversity of biological types and sizes, from small forms, comparable to rodents, to giants with no analogues in modern faunas. Having been all of them traditionally considered herbivores, this diversity is reflected in different morphologies of the masticatory apparatus, suggesting a variety of feeding habits.

The application of biomechanics to the study of the masticatory apparatus of fossil mammals is a convenient approach to test functional hypotheses. Jaws act as a third class lever system, with the input force ($F_i$) crossing the lever between the pivot and output force ($F_o$). The temporomandibular joint (TMJ) acts as a pivot, the masticatory muscles provide the input force, and the output force is produced by the teeth acting on food (Fig. 2) (Maynard Smith and Savage 1959; Crompton and Hiiemae 1969; Greaves 1974; Hildebrand 1988). The perpendicular

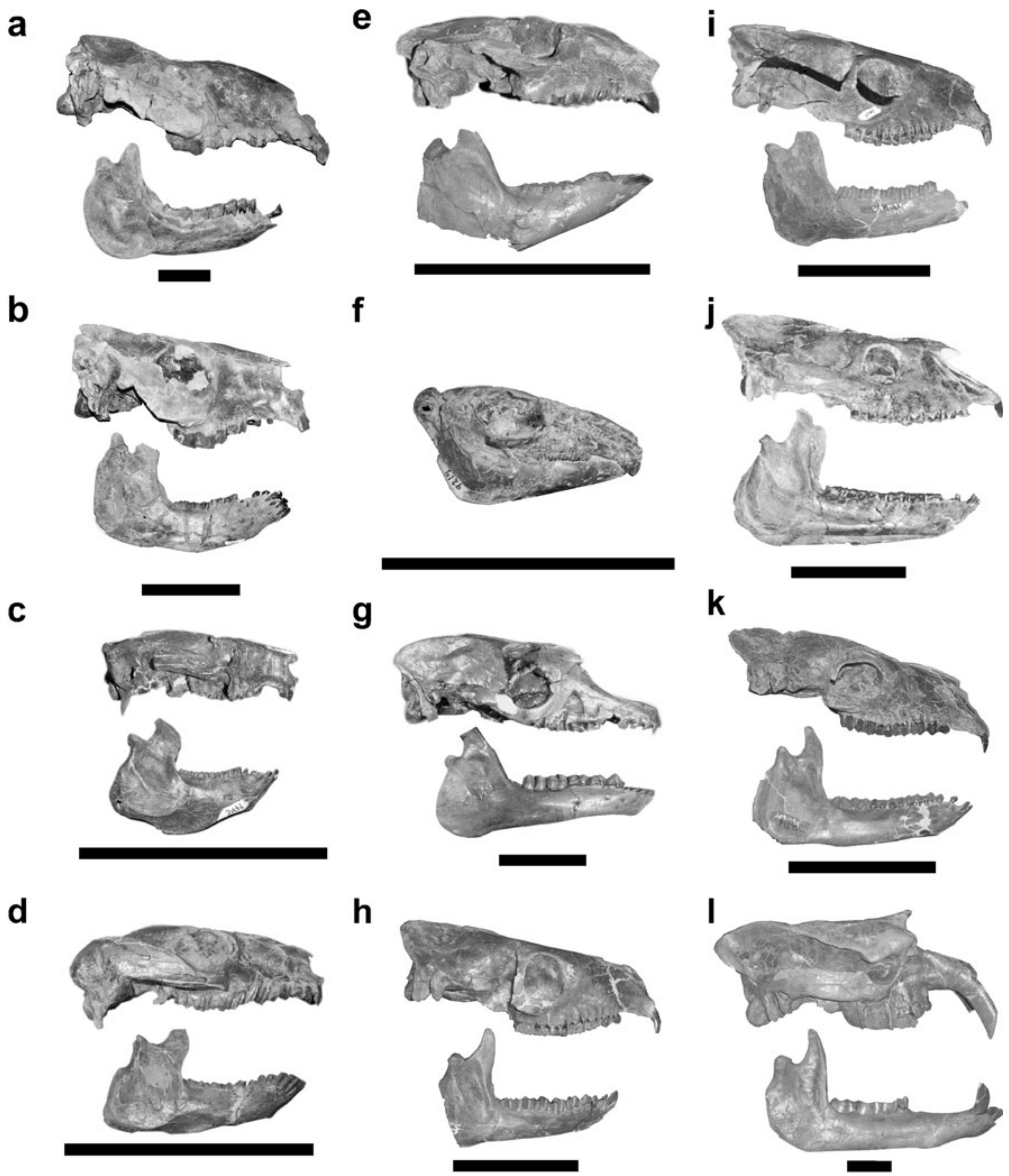

**Fig. 1** skulls of Santacrucian ungulate taxa. Toxodontidae: **a** *Nesodon*, MPM-PV 4377 (cranium) and MPM-PV 3659 (mandible); **b** *Adinotherium*, MPM-PV 3532 (cranium) and 3666 (mandible); Typotheria: **c** *Interatherium*, MPM-PV 3471; **d** *Protypotherium*, AMNH 9868; **e**, *Hegetotherium*, MPM-PV 3526 (cranium) YPM-PU 15298 (mandible); and **f** *Pachyrukhos*, AMNH 9219; Macraucheniidae: **g** *Theosodon*, MACN-A 9284–88; Proterotheriidae: **h** *Anisolophus*, YPM-PU15368 (cranium) YPM-PU 15996 (mandible); **i** *Tetramerorhinus*, MPM-PV 3493 (cranium) YPM-PU 15436 (mandible); **j** *Diadiaphorus*, MPM-PV 3397; **k** *Thoatherium*, MPM-PV 3529 (cranium) YPM-PU 15719 (mandible); Astrapotheria: **l** *Astrapotherium*, AMNH 9278. Scale bar =10 cm

distances between the action line of the forces (muscle force and bite force) and the pivot is a segment of the lever, respectively called the input moment arm ($M_i$) and output moment arm ($M_o$) (Fig. 2). For instance, when the masseter contracts and pulls the mandibular angle, it generates a closing force ($F_i$) and the input moment arm ($M_i$) corresponds to the perpendicular length between the pivot and the line of action of the muscle. The output moment arm ($M_o$) is the perpendicular segment from the temporomandibular joint to the point where the bite is applied on

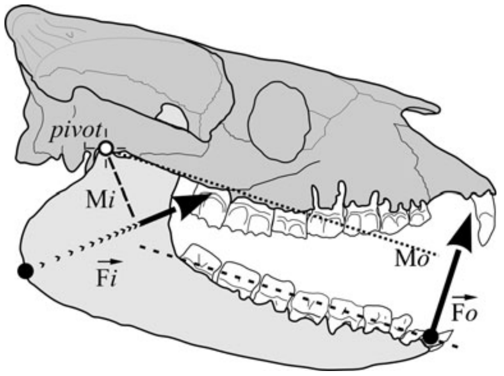

**Fig. 2** jaws act as a third class lever system during masseter contraction, shown in a *Diadiaphorus* skull. Abbreviations: $F_i$, input force vector; $F_o$, output force vector; $M_i$, input moment arm; $M_o$, output moment arm

the dental series (Fig. 2). So when the system is in equilibrium, it satisfies the equation

$$F_iM_i = F_oM_o$$

which shows that to produce an increase in the $F_o$, while maintaining $F_i$ constant, Mi should be increased or Mo reduced.

The analysis of the lever system and the relationship between moment arms (in a static equilibrium) allows us to evaluate whether the mechanical advantage of the system favors the development of strength or speed. To achieve this goal, action lines of input forces need to be known. This is practical on living mammals, but a rather difficult task on fossils specimens. To deal with this obstacle and to enable comparison between fossils and living animals, Vizcaíno et al. (1998) proposed a geometric model that was applied to fossil armadillos (Vizcaíno et al. 1998; De Iuliis et al. 2000; Vizcaíno and De Iuliis 2003), ground sloths (Bargo and Vizcaíno 2008), and that was modified to apply to extinct archosaurs (Desojo and Vizcaíno 2009). The geometric model requires reconstruction of the areas of origin and insertion of the masticatory muscles. Vizcaíno et al. (1998) drew lines of action for the temporalis and masseter representing several realistic orientations in the sagittal plane and measured moment arms to each line of action. They estimated the moment arm of each muscle as the mean of several estimations of moment arms for that muscle. To determine realistic orientations for each line of action, they used the most anterior and posterior extent of the origin and insertion muscle scars, and different points within the origin and insertion areas of each muscle.

In this contribution, a geometric morphometric (GM) approach inspired by Vizcaíno et al. (1998) is applied to estimate muscle moment arms in a static 3D bite model based on 3D landmarks and semilandmarks of crania with mandibles in occlusion. To evaluate the consistency of the model, a test sample of different diet categories of extant mammals was applied previously to the application on ungulate fossil assemblage. Consequently, the goal of this work is to propose a new 3DGM method to evaluate jaw mechanics, prove its reliability, and apply it to test functional hypotheses about dietary resource use that were generated by previous ecomorphological studies (Townsend and Croft 2008; Cassini et al. 2011) on three orders of Santacrucian ungulates (Notoungulata, Litopterna, and Astrapotheria).

## Materials and Methods

### Acronyms

AMNH: American Museum of Natural History, New York, USA; MACN: Museo Argentino de Ciencias Naturales "Bernardino Rivadavia," Buenos Aires, Argentina; MLP: Museo de La Plata, La Plata, Argentina; MPM-PV: Museo Regional Provincial Padre "M. J. Molina," Río Gallegos, Argentina; YPM-PU: Yale Peabody Museum, New Haven, USA.

### Data

Twenty-five specimens of Santacrucian ungulates were analyzed. Only specimens with cranium and mandible belonging to the same individual, and no or little apparent deformation, were selected. They include seven toxodontids and nine typotheres (Notoungulata), five proterotheriids and two macraucheniids (Litopterna), and two astrapotheres (Astrapotheria) (see Appendix 1). The test sample used to evaluate the consistency of results and as a reference framework consists of skulls of eight specimens of extant carnivorous, omnivorous, and herbivorous mammals, which were digitized in occlusion (Appendix 2).

### Masticatory Muscle Reconstruction

Reconstruction of the masticatory muscles involves identifying areas of origin and insertion based on bone scars. Witmer (1995) proposed a method called the "extant phylogenetic bracket" (EPB) to make inferences about soft tissues not preserved in the fossil record. Two living taxa constitute the "bracket" within which the fossil taxon is phylogenetically contained. This procedure assumes the correlation between bone-soft feature in living taxa and that this relationship is due to common ancestry. If the bone trait is present in the fossil, then the optimizations can hypothesize with varying degrees of confidence about the implications of the presence or absence of the soft feature.

Although the use of the EPB approach is very recommendable, as mentioned above the families of

Santacrucian ungulates have no modern descendants and their phylogenetic position within mammals is still discussed, rendering this EPB methodology inapplicable. Therefore, we used a more traditional approach (as in De Iuliis et al. 2000; Vizcaíno and De Iuliis 2003; Bargo and Vizcaíno 2008) based on general descriptions of mammals with different types of diets by Turnbull (1970) complemented with our own dissections performed on different groups of living mammals (the pig *Sus scrofa*, the rabbit *Oryctolagus cunniculus*, the pampas deer *Ozotoceros bezoarticus*, and the white-eared opossum *Didelphis albiventris*). When appropriate and possible, nomenclature for the descriptions follows the Nomina Anatomica Veterinaria (World Association of Veterinary Anatomists, International Committee on Veterinary Gross Anatomical Nomenclature), as recently has been applied to the Notoungulata (Gabbert 2004) and Pyrotheria (Billet 2010), and complemented with the illustrated guide of Schaller (2007).

## Landmark Data

The three-dimensional landmark coordinates were acquired with a Microscribe G2L digitizer; they are defined in Tables 1 and 2 and shown in Fig. 3. Both sides and midline landmarks were included as they are necessary for a better digital articulation of the cranium and mandible (see next section). They comprise 44 cranial and 18 mandibular landmarks including type I, II, and III or semilandmarks (Table 1 and 2). The semilandmarks were used to capture the origin and insertion scars, based on the reconstruction of the origin and insertion areas of the temporal and masseter muscles, each one taken as a whole unit. On the cranium, semilandmarks were placed over the ventral margin of the zygomatic arch (masseter origin; L12 to 16; Table 1 and Fig. 3b–c), supramastoid crest, nuchal crest, and sagittal crest (or temporal line) (L1 to 8; Table 1 and Fig. 3b–c). On the mandible, semilandmarks were placed over the caudal border of the mandibular angle along the masseter scar (L14 to 18; Table 2 and Fig. 3c), and along the rostral border of coronoid process over the scar of the temporalis muscle (L7 to 11; Table 2 and Fig. 3c). These semilandmarks were resampled and reduced in number to five equispaced (as total) using "resample" software of NYCEP (Reddy et al. 2007).

## Articulation of Fossil Specimens

To calculate the lever arms, cranium and jaw must be articulated. Fully complete and articulated cranium and jaws are rarely seen in the fossil record. In addition, some deformation is usually present, making it difficult to articulate both elements manually for scanning the specimens without compromising the integrity of the fossil. In order to avoid these complications, articulation of these

**Table 1** Cranial landmarks, names and definitions used in the present study

| Number | Name | Definition of landmark |
|---|---|---|
| 1 & 25 | | anteriormost origin of m. temporalis on the arcus zygomaticus |
| 2–3 & 26–27 | semilandmarks | m. temporalis origin on os temporale pars squamosa |
| 4 & 28 | | sutura temporooccipitalis on the crista supramastoidea |
| 5–7 & 29–31 | semilandmarks | m. temporalis origin along the crista sagittalis or linea temporalis |
| 8 & 32 | Stephanion | sutura coronalis at the intersection with the linea temporalis |
| 9 & 33 | Dacryon | sutura zygomaticolacrimalis at the margo orbitalis |
| 10 & 34 | | inner edge of the tuberculum articulare |
| 11 & 35 | | outer edge of the tuberculum articulare |
| 12 & 36 | | caudal margin of the crista facialis on the sutura zygomaticotemporale |
| 13–15 & 37–39 | semilandmarks | m. masseter origin along the crista facialis |
| 16 & 40 | | anteriormost origin of m. masseter |
| 17 & 41 | | distal margo alveolare of the last molar |
| 18 & 42 | | margo interalveolaris between the last premolar and first molar |
| 19 & 43 | | mesial margo alveolare of the first functional premolar |
| 20 & 44 | | distal margo alveolare of the last incisor or horny pad scar |
| 21 | Nasion | sutura frontonasalis on the sagittal plane |
| 22 | Rhinion | rostral edge of the os nasale on the sutura internasalis |
| 23 | Nasospinale | sutura interincisiva on the mid-sagittal plane of the nasal aperture |
| 24 | Prosthion | sutura interincisiva on the margo alveolaris |

Table 2 Mandibular landmarks, names and definitions used in the present study

| Number | Name | Definition of landmarks |
|---|---|---|
| 1 | Gnathion | caudo-ventral margin of the mandibular symphysis on the midline |
| 2 | Infradentale | alveoli dentalis of i1 on the midline |
| 3 | | distal margin of alveoli dentalis of the last lower incisor |
| 4 | | mesial margin of the alveoli dentale of the first functional premolar |
| 5 | | margo interalveolaris between the last premolar and first molar |
| 6 | | distal margin of the alveoli dentale of the last molar |
| 7 | | anteriormost point of the scar of the m. temporalis insertion on the ramus mandibulae |
| 8–10 | semilandmarks | scar of the m. temporalis insertion on the ascending process of the ramus mandibulae |
| 11 | | posteriormost point of the scar of the m. temporalis insertion on the processus coronoideus |
| 12 | Condylion lateral | most lateral margin of the mandibular condyle |
| 13 | Condylion medial | most medial margin of the mandibular condyle |
| 14 | | most dorsal-caudal rugosity from m. masseter insertion |
| 15–17 | semilandmarks | caudal border of the angulus mandibulae along m. masseter scar |
| 18 | | most anterior roughness from m. masseter insertion |

elements was performed digitally. The articulation procedure was performed as follows:

a. Landmark selection. The landmarks (Fig. 3) used as reference in the skull and jaw were the mesial edge of the first functional premolar (L19 cranium and L4 mandible), the rear edge of the last molar (L17 cranium and L6 mandible), the outer and inner edge of the articular condyle of the mandible (processus condylaris; L12 and L13 respectively), and the outer and inner edge the articular tubercle (tuberculum articulare) in the glenoid cavity (L11 and L10 respectively).
b. Reflection. Since normally there is only one hemimandible preserved, or the two fail to show the same degree of preservation, the most complete hemimandible was reflected in the plane of symmetry defined by the mandibular symphysis. To do so, we used the R-function AMP.r written by Annat Haber, University of Chicago (available online at http://life.bio.sunysb.edu/morph/; see also Online Resource 1).
c. Articulation process. The digital articulation was performed with R-function unifyVD.r written by Annat Haber, University of Chicago (available online at http://life.bio.sunysb.edu/morph/; see also Online Resource 2) to unify the dorsal and ventral views scanned separately. This script binds both configurations of landmarks using the landmarks selected in (**a**) to obtain a new landmark configuration with the whole form (cranium and mandible articulated), by mean of Procrustes superposition.
d. Articulation adjustment. The articulation integrity obtained was evaluated graphically and analytically, comparing the distances from the outer edges of the processus condylaris of the mandible and the articular tubercle of the skull. If the bicondylar width (cdl-cdl) is larger or smaller than the width at the articular tubercles, it is adjusted by a rotation of the symphyseal axis using an R script (see Online Resource 3), and then the process of articulation described in (c) is repeated.

## Moment arm Calculation

Moment arms were calculated by means of an orthogonal projection (Fig. 4) of a triangle in R3 defined with a fixed vertex on the pivot (P; landmark 12 of the mandible) and the other two movable along the origin (O) and insertion (I) muscle scars. Starting with $O_1$ as the most anterior origin of the muscle scar, and $I_1$ as the most anterior insertion of the muscle (exemplified by the masseter in Fig. 4), five positions of O ($O_1$, …, $O_5$) along the origin scar and five positions of I ($I_1$, …, $I_5$) along the insertion scar are anchored to the corresponding semilandmarks. Then, a vector $u$ (representing the line $O_1P$) and a vector $w$ (representing the lines $O_1I_1$) were used to calculate the perpendicular distance ($h$) between the pivot (P) and the line $O_1I_1$. The distance $h$ is the lever arm of the input force, with a line of action defined in the same direction and opposite to the vector $w$. For each $O_i$ five vectors $w$ were calculated (representing the lines $O_iI_1$, …, $O_iI_5$) and the corresponding $5h$ distances; therefore, $25h$ distances were calculated for each muscle, which correspond to the lever arm for each line of action hypothesized. The mean of these 25 lever arms is the estimated mean muscle moment arm. This procedure is repeated for both the masseter and temporalis muscle, where each of the five semilandmarks describes the origin and insertion of these muscles.

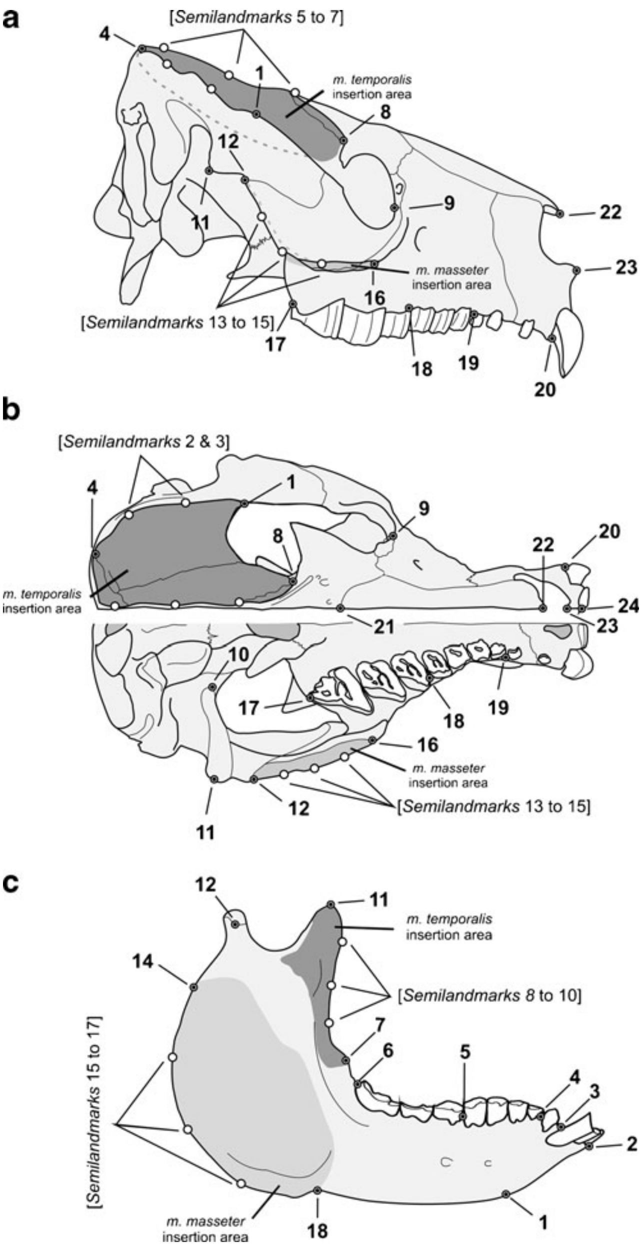

**Fig. 3** landmarks (also see Table 1 and 2). *Adinotherium* cranium and mandible showing the landmarks on the right side and midline. Inferred origin and insertion areas for masseter and temporalis are also shown

Output force lever arms were calculated as the perpendicular distances from the pivot to different vectors perpendicular to the occlusal plane of the mandibular teeth. These output forces are applied to the most anterior margin of the mandibular symphysis (infradentale; L2), the first functional premolar (L4), margo interalveolaris between the last premolar and first molar (L5), and last molar (L6). The occlusal plane is defined as the one containing the mesial and distal edges of the mandibular tooth of each hemimandible, being the minimum Procrustes distance to each point. Then the distances between the pivot and each bite point were calculated as the distance parallel to the plane (see Online Resource 4).

## Results

### Masticatory Muscle Reconstruction

A full detailed description of the genera here studied was made by Cassini (2011). In this section we focus on the anatomical traits enabling us to infer the origin and insertion areas of the two main masticatory muscles (temporalis and masseter).

Among Notoungulata, the toxodontids *Adinotherium* and *Nesodon* belong to the subfamily Nesodontinae, which is the most generalized members of the family (Bond and García 2002). Scott (1912) pointed out that their morphology is quite conservative and that it is difficult to find tangible differences between these genera. In both genera the temporalis is well developed, which is evident from the strong crests (sagittal, nuchal, and supramastoid) delimiting a great temporal fossa. The zygomatic process of the temporal bone has an extensive surface where the zygomatic temporalis could have its origin. This muscle is present in all mammals but more developed in carnivores and generalized herbivores sensu Turnbull (1970). On the mandible the insertion of m. temporalis pars superficialis covers the low coronoid process, the pars profunda runs along the rostral margin of the rugosity on the mandibular angle, and the zygomatic temporalis attaches over the concave depression below m3; the whole muscle considered as a unit is depicted in Figs. 3 and 5a.

Both *Adinotherium* and *Nesodon* have a similar great development of masseter, which becomes more evident by the extensive surface available for the insertion along the rugosity of the ventral and caudal margin of the mandibular angle and the lateral surface of the ramus (Figs. 3, 5a). This configuration is similar to extant herbivorous mammals. In addition, the m. zygomatico-mandibularis sensu Turnbull (1970) could constitute an important part of the musculature, which is suggested by a tall and robust zygomatic arch.

Muscular reconstructions for Typotheria include the two Santacrucian interatheriids *Protypotherium* and *Interatherium* plus the hegetotheriid *Pachyrukhos*. Both interatheriids have a great temporal fossa delimited by the temporal line in the frontal bone and the sagittal, nuchal, and supramastoid crests, which suggest a well-developed temporalis. However, temporalis seems to be greater in *Interatherium*. The dorsal surface of the pars squamosa from the temporal bone is long and narrow rostrocaudally, suggesting a small origin area for the zygomatic temporalis and consequently the muscle was probably poorly developed. In the mandible a great area for the insertion of the temporalis is suggested by the high and wide coronoid process.

The rugosity in the crista facialis, along the ventral side of the zygomatic process of the maxilla, suggests a long anteroposterior origin area for the masseter for both interatheriids. *Interatherium* has a long descending process of the maxilla just below the orbit over the anterior-most scar of the masseter origin, causing it to project down into the occlusal plane. In the mandible both interatheriids have an extensive surface available for the insertion of the masseter. However, in *Protypotherium* the caudal margin is displaced caudally beyond the temporomandibular joint (Fig. 5b–c).

In contrast to interatheriids, the temporalis was probably poorly developed in the hegetotheriid *Pachyrukhos*. It possesses a large orbit and the posterior temporal fossa was reduced, so there is a small origin area for the temporalis. On the mandible, scars on the ascending process of the mandibular angle and a reduced coronoid process suggest a small area for the insertion of the temporalis. The crista facialis extends along the ventral side of the orbit, because the zygomatic arch is reduced and forms the caudal margin of the orbit. Those features suggest a long, anteroposteriorly bent masseter origin area along the ventral margin of the orbit. In the mandible the mandibular angle is well developed and the rugosity on the caudal margin suggests a great extension of the insertion area for the masseter. This muscle is anteriorly extended beyond the temporomandibular joint. Both muscles areas considered as a unit are depicted in Fig. 5d.

Among Litopterna, the macraucheniid *Theosodon* has a greatly developed temporal fossa. It is well delimited by a strong temporal line on the frontal bone and the sagittal, nuchal, and supramastoid crests. In addition, the facies temporalis of pars squamosa of the temporal bone plus the parietal bone form a great area for the origin of the temporalis, suggesting a great development of this muscle. The dorsal surface of the pars squamosa from the temporal bone is long and narrow rostrocaudally, suggesting a small origin area for the zygomatic temporalis and consequently it was probably poorly developed. On the mandible, the scar on the rostral margin of the mandibular angle and the great extent of the coronoid process, which is high and caudally curved, provide a large area for the insertion of the temporalis. The masseter origin runs along the rugosity in the crista facialis below the orbit and the ventral side of the zygomatic process of the maxilla. On the mandible the scar

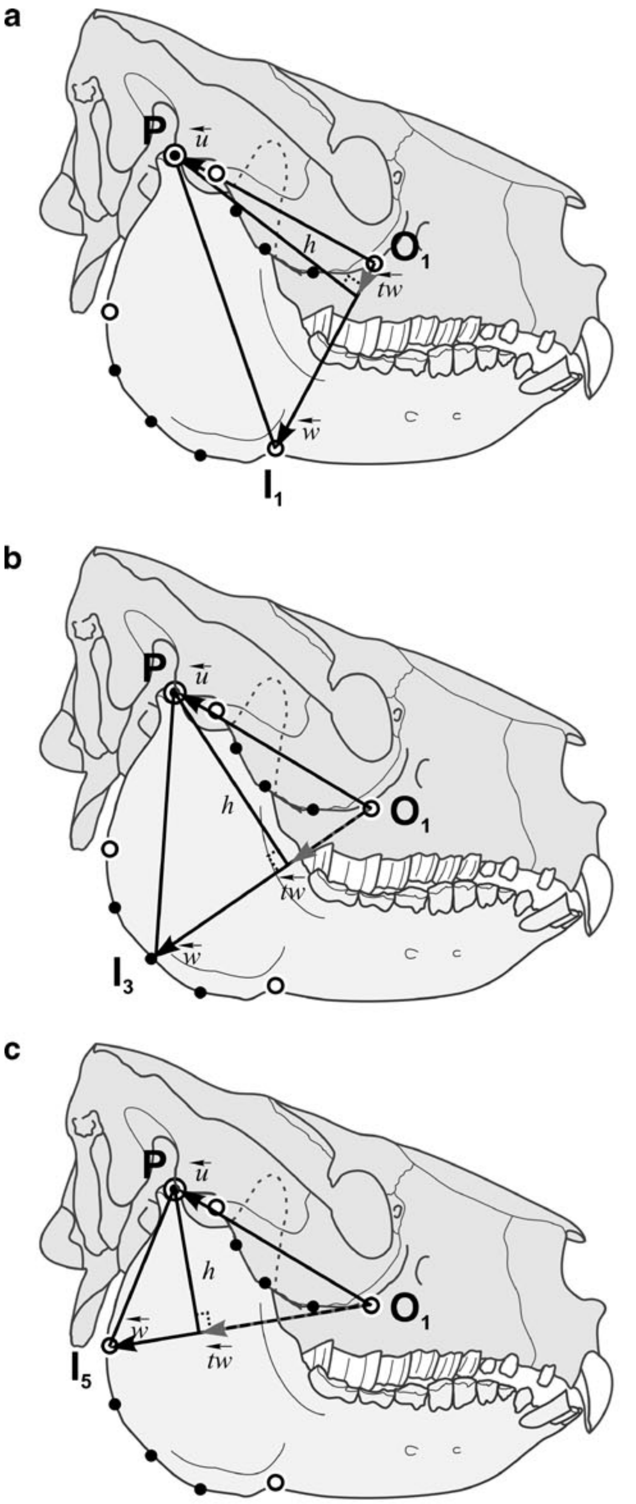

**d**

$$\overleftarrow{u} = \overline{O_i P} \qquad \overleftarrow{w} = \overline{O_i I_j}$$

$$\overleftarrow{tw} = \text{proy}_{\overleftarrow{w}}\, \overleftarrow{u} = \frac{\overleftarrow{w} \cdot \overleftarrow{u}}{\overleftarrow{w} \cdot \overleftarrow{w}}\, \overleftarrow{w} \qquad h = \left\| \overleftarrow{u} - \overleftarrow{tw} \right\|$$

**Fig. 4** **a**–**c** first and intermediate steps used to calculate the mean moment arm of masseter exemplified by *Adinotherium ovinum*. See details in the text. **d** vector definitions and formulae to calculate each *h* distance

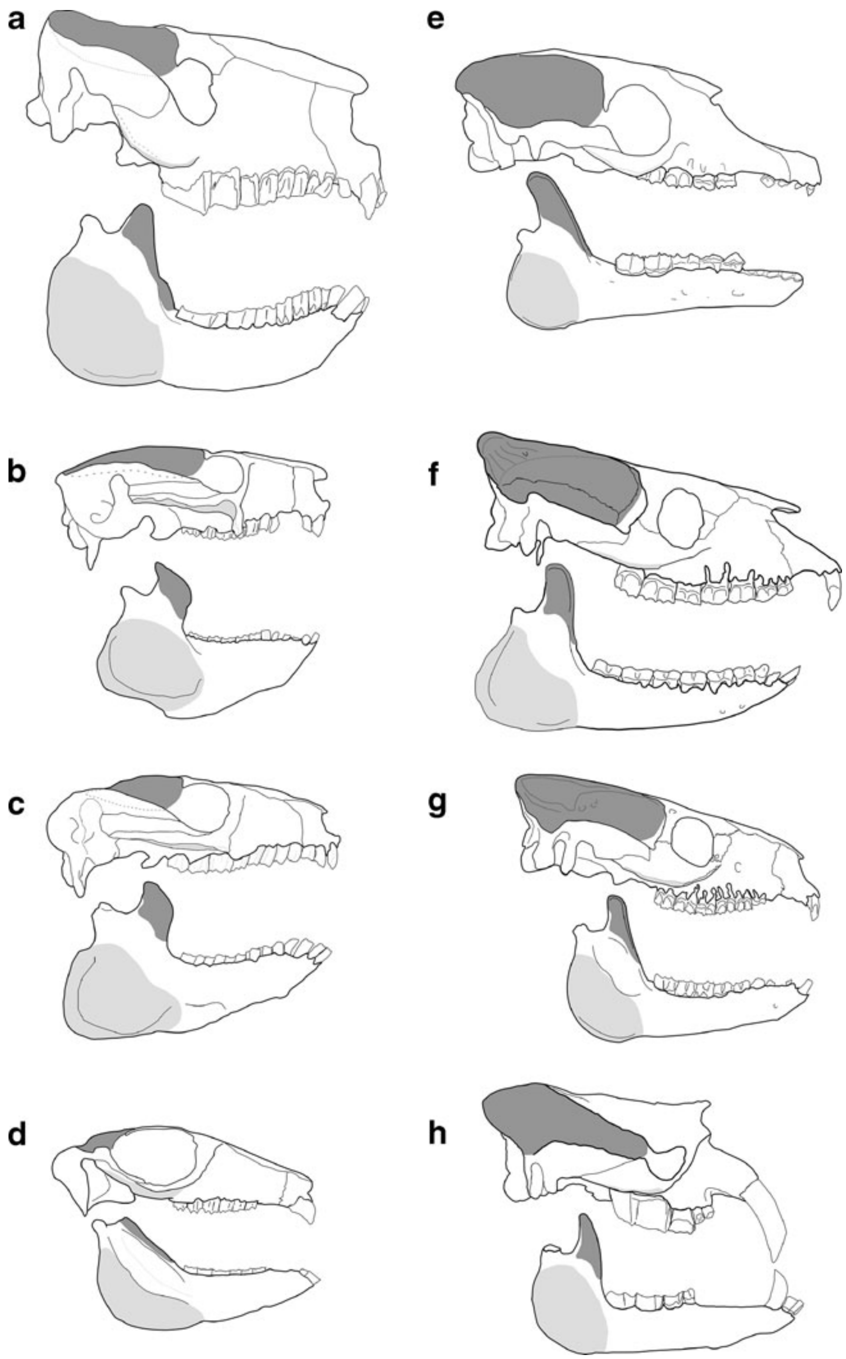

**Fig 5** origin and insertion areas of the two masticatory muscles (temporalis dark gray, and masseter pale gray) shown on skulls of **a** *Nesodon*; **b** *Interatherium*; **c** *Protypotherium*; **d** *Pachyrukhos*; **e** *Theosodon*; **f** *Diadiaphorus*; **g** *Tetramerorhinus*; and **h** *Astrapotherium*

on the caudal margin and the lateral surface of the mandibular angle provides a great area for the insertion of the masseter. Both muscles areas are show in Fig. 5e.

Among proterotheriids, both genera studied, *Diadiaphorus* and *Tetramerorhinus,* show a similar pattern for the inferred masticatory muscles. The temporal fossa is well developed as indicated by a strong temporal line on the frontal, the sagittal, nuchal, and supramastoid crests and the extension of facies temporalis of pars squamosa of the temporal bone plus the parietal, which are caudally directed beyond the occiput. These features indicate a great area for the origin of a well-developed temporalis muscle. On the mandible the attachment area for the insertion runs along the ascending process of the mandibular angle and extends over the coronoid process, which is high and slender. The masseter origin takes place in the roughness of the crista facialis caudal to the orbit and mainly on the ventral side of the zygomatic process of the maxilla. This origin area becomes short, because it is restricted by a small extension of the infratemporal fossa. In the mandible both proterotheriids have extensive caudal roughness of the mandibular angle that almost reaches the collum mandibulae of the processus condylaris, as well as, a

**Table 3** Descriptive statistics [Mean±*standard deviation* (*n*)] for moment arms (millimeters) of input and output forces for each masticatory muscle and bite point along mandible

| Genera (*n*) | Masseter | Temporalis | Infradentale | First premolar | Premolar / molar | Last molar |
|---|---|---|---|---|---|---|
| *Astrapotherium (2)* | 88.537±15.438 | 84.300±16.770 | 432.322±56.354 | 252.075±41.708 | 224.656±46.193 | 113.744±6.564 |
| *Diadiaphorus (4)* | 38.194±4.485 | 37.550±5.765 | 187.325±6.825 | 166.822±5.130 | 106.461±2.841 | 55.220±5.731 |
| *Tetramerorhinus (1)* | 34.772 | 31.210 | 150.901 | 128.956 | 83.915 | 47.412 |
| *Theosodon (2)* | 40.847±2.852 | 40.684±8.309 | 235.001±13.953 | 197.941±9.337 | 124.959±10.270 | 57.961±10.132 |
| *Adinotherium (3)* | 45.042±4.411 | 54.734±6.031 | 186.611±17.754 | 153.085±18.214 | 110.847±15.121 | 63.723±3.309 |
| *Nesodon (4)* | 90.108±9.095 | 98.517±20.025 | 348.412±26.708 | 297.935±24.819 | 237.035±25.395 | 123.473±15.904 |
| *Protypotherium (3)* | 16.485±2.007 | 20.155±4.917 | 75.640±8.154 | 62.094±6.112 | 45.553±7.598 | 25.160±3.021 |
| *Interatherium (5)* | 13.177±2.866 | 16.111±1.230 | 59.113±5.197 | 44.439±4.595 | 32.950±4.742 | 20.125±2.292 |
| *Pachyrukhos (1)* | 16.118 | 8.242 | 60.621 | 46.070 | 35.357 | 20.609 |
| *Chrysocyon (1)* | 30.306 | 39.422 | 172.513 | 132.494 | 79.629 | 58.958 |
| *Puma (1)* | 44.975 | 39.043 | 138.990 | 102.222 | 64.605 | 62.767 |
| *Hippocamelus (1)* | 49.589 | 28.375 | 232.277 | 138.933 | 101.294 | 56.609 |
| *Camelus (1)* | 70.995 | 76.494 | 378.543 | 289.896 | 184.646 | 88.146 |
| *Lama (1)* | 65.219 | 42.028 | 242.890 | 144.349 | 125.494 | 64.346 |
| *Sus (1)* | 50.148 | 37.943 | 297.257 | 193.707 | 143.735 | 80.026 |
| *Equus (1)* | 125.506 | 65.746 | 450.010 | 321.065 | 224.809 | 140.132 |
| *Tapirus (1)* | 75.864 | 61.265 | 285.885 | 193.457 | 122.558 | 84.897 |

great surface available for the insertion of the masseter. However, in *Diadiaphorus* the caudal margin is displaced caudal to the temporomandibular joint whereas in *Tetramerorhinus* it is anteriorly directed (Figs. 5f–g).

The astrapothere (*Astrapotherium*) has a long, rostrocaudally directed temporal fossa. Caudal to the orbit, it is enclosed by the lateral expansion of the frontal and parietal and becomes larger in the posterior region. This suggests a great temporalis that is very well developed caudally. On the mandible, a high, subtriangular coronoid process and rugosity on the rostral margin of the mandibular angle suggest the insertion of a well-developed temporalis. The rostral margin of the crista facialis shows a wide scar that becomes narrow caudally, extending over the ventral margin of the temporal process of the zygomatic bone. On the mandible, the rugosity along the caudal margin of mandibular angle and the lateral surface suggests an extended area for the insertion of masseter. Both muscle areas considered as a unit are depicted in Fig. 5h.

## Masticatory Biomechanics

Calculated moment arms for each muscle and four different bite points are listed in Table 3. The relationships between input and output force moment arms for both muscles acting alone and together are listed in Table 4. Considering both muscles acting together, for the resultant force (sum of both forces; see Duarte and Riestra 2004) the estimated resultant moment arm was computed as the mean of both muscles moment arms. The control sample and the Santacrucian ungulates are treated separately in the results and discussion sections (see below). Note that across all mammals examined here, and consistent with a model of a third class lever system, none of the input force moment arms (muscles) was higher than the output forces moment arms (bite points) either in absolute value (Table 3) or ratio (lower than one; Table 4). Considering both muscles acting together, ratios between input and output moment arms were also lower than one (Table 4).

### *Control Sample*

Results in the control sample were consistent with biomechanical expectations. Table 3 shows the average moment arms of the 3D geometric method. For carnivores the masseter and temporalis moment arms are somewhat similar, but for herbivores (except the dromedary) the masseter moment arm is approximately twice that of the temporalis moment arm. By contrast, the temporalis lever arm of carnivores was equal or up to 1.3 times greater than that of masseter. For the boar, an omnivore, this ratio is about 1.25. Among the herbivores (the tapir and the camelids), the temporalis has an especially long lever arm (Table 3).

The puma has the highest ratios between input and output lever arm of both muscles alone and acting together over the muzzle (i.e., infradentale, Table 4). In addition, it has higher values along the entire dentition than the maned wolf, except at the distal edge of the last molar when only the temporalis was considered (Table 4). Among herbivores, with the exception of the dromedary biting at the last molar, masseter lever arms were always higher those of temporalis (Table 4). The tapir configuration deserves mention: mechanical advantage for both muscles acting alone and together, and at bite points along the molar tooth row, is even greater in the tapir than in the puma (Table 4).

### *Santacrucian Ungulates*

The average lever arms of each muscle are shown in Table 3. Among Santacrucian ungulates, only the notoungulate *Pachyrukhos* has a masseter lever arm greater than the temporalis (Table 3). In the remaining genera, masseter and temporalis are similar, the former being slightly greater in the astrapothere and litopterns and the latter slightly greater in notoungulates (Table 3).

Leverages are listed in Table 4. In general, notoungulates (with the exception of *Pachyrukhos*) show higher values of relative lever arms for both muscles than litopterns. Considering both muscles acting together, *Adinotherium* and *Nesodon* show the highest values of all Santacrucian ungulates at the muzzle. This result is similar to that of the puma (~0.27; Table 4). Also, *Adinotherium* and *Nesodon* have the highest leverage values at the molar tooth row. Nesodontines and interatheriids have better mechanical advantage for the temporalis than the masseter. By contrast, the hegetotheriid *Pachyrukhos* shows a greater leverage for the masseter.

## **Discussion**

The Greek mathematician, Archimedes (*c.* 287 BC−*c.* 212 BC), produced an explanation of the principle of the lever, a mechanism of force transfer with a stiff beam across a rotation point, or fulcrum, that may enhance either force or speed at the end of the beam. The study of the masticatory mechanics and morphology of the temporomandibular joint allows us to assess the overall capacity of the masticatory apparatus as a lever system (Maynard Smith and Savage 1959; Greaves 1988; Vizcaíno et al. 1998; Bargo and Vizcaíno 2008). At least two factors affect the performance of a system of levers: design and input force. Output force may thus be increased by improvement of the design—thereby rendering the apparatus more efficient in transference of input force—and by increasing the input force (De Iuliis et al. 2000). The relationship between muscle lever arms and output arms (at each bite point) allows us to detect design differences, which indicate a preponderance of force over speed in jaw closing or vice versa (Vizcaíno and Bargo 1998; Vizcaíno et al. 1998, 2006; Bargo 2003).

In this contribution we analyzed the lever system of the masticatory apparatus extending the two-dimensional geometric model proposed by Vizcaíno et al. (1998) to a three-dimensional approach. In doing so, we selected a control sample consisting of herbivorous, omnivorous, and carnivorous extant mammals for the analysis of the results of the Santacrucian ungulates masticatory system.

### Masticatory Biomechanics in the Control Sample

Results in the control sample were consistent with biomechanical expectations, with longer lever arms for the masseter than for the temporalis in herbivores, and with longer lever arms for the temporalis than for the masseter in carnivores (Maynard Smith and Savage 1959; Greaves 1985; Hildebrand 1988; Covey and Greaves 1994).

However, the relationships of the input and output lever arms at various points along the dental series, considering both muscles separately and then together, require a more comprehensive analysis. For example, among carnivores the relative strength resulting from masseter and temporalis lever arms at the end of the muzzle (when compared with each other or considered together) is greater in the puma than in the maned wolf in concordance with the results of the classical work of Radinsky (1981). Based on the difference between the two classical models for prey capture between felids and canids (see Christiansen and Adolfssen 2005 and references therein), it seems clear that the puma is designed for force enhancement. On the contrary, and considering that third order lever systems are better designed for speed (see Westneat 2003), the maned wolf could benefit from a fast closing muzzle to capture and kill small faster prey (e.g., rodents and birds; see diet composition on Aragona and Setz 2001).

Among herbivorous mammals, except the dromedary, the relative lever arms of the masseter are always longer than those of the temporalis. As Greaves (1974, 1995) pointed out, although the condyle is also well elevated, this is not the reason for a improvement for masseter (see below): simultaneous occlusion along the tooth row is the most important reason for high condyles in herbivores. Instead, the leverage of the masseter would improve through an anterior displacement of its origin (Greaves 1974, 1995). Considering only the masseter, in forms with great development of this muscle like the horse (a grazer), the relative moment arms are larger than for the huemul (the Andean deer, a browser). On the other hand, when the temporalis lever arms are evaluated, the values at the different bite points were very similar for the horse and the huemul. Greaves (1991) stated that the majority of ungulates have an anteriorly-directed muscle resultant. Although, some exceptions to this model were found by Greaves (1991), among ungulates the dromedary has a

**Table 4** Leverage along the mandible

| Genera | M. masseter | | | | M. temporalis | | | | M. masseter + M. temporalis | | | |
|---|---|---|---|---|---|---|---|---|---|---|---|---|
| | Infradentale | First premolar | Premolar molar | Last molar | Infradentale | First premolar | Premolar molar | Last molar | Infradentale | First premolar | Premolar molar | Last molar |
| *Astrapotherium* | 0.204 | 0.351 | 0.395 | 0.776 | 0.194 | 0.333 | 0.376 | 0.738 | 0.199 | 0.342 | 0.385 | 0.757 |
| *Diadiaphorus* | 0.204 | 0.229 | 0.359 | 0.703 | 0.201 | 0.225 | 0.353 | 0.687 | 0.202 | 0.227 | 0.356 | 0.695 |
| *Tetramerorhinus* | 0.230 | 0.270 | 0.414 | 0.733 | 0.207 | 0.242 | 0.372 | 0.658 | 0.219 | 0.256 | 0.393 | 0.696 |
| *Theosodon* | 0.174 | 0.206 | 0.327 | 0.711 | 0.172 | 0.205 | 0.324 | 0.700 | 0.173 | 0.206 | 0.325 | 0.706 |
| *Adinotherium* | 0.242 | 0.296 | 0.410 | 0.706 | 0.296 | 0.363 | 0.503 | 0.864 | 0.269 | 0.329 | 0.456 | 0.785 |
| *Nesodon* | 0.260 | 0.305 | 0.385 | 0.741 | 0.281 | 0.329 | 0.415 | 0.799 | 0.271 | 0.317 | 0.400 | 0.770 |
| *Protypotherium* | 0.218 | 0.268 | 0.351 | 0.654 | 0.283 | 0.347 | 0.455 | 0.848 | 0.241 | 0.294 | 0.402 | 0.726 |
| *Interatherium* | 0.228 | 0.302 | 0.405 | 0.663 | 0.275 | 0.364 | 0.492 | 0.798 | 0.247 | 0.329 | 0.447 | 0.728 |
| *Pachyrukhos* | 0.266 | 0.350 | 0.456 | 0.782 | 0.136 | 0.179 | 0.233 | 0.400 | 0.201 | 0.264 | 0.344 | 0.591 |
| *Chrysocyon* | 0.181 | 0.213 | 0.323 | 0.524 | 0.235 | 0.277 | 0.420 | 0.681 | 0.208 | 0.245 | 0.371 | 0.603 |
| *Puma* | 0.313 | 0.398 | 0.529 | 0.671 | 0.272 | 0.345 | 0.460 | 0.583 | 0.292 | 0.372 | 0.495 | 0.627 |
| *Hippocamelus* | 0.211 | 0.331 | 0.439 | 0.858 | 0.121 | 0.189 | 0.251 | 0.491 | 0.166 | 0.260 | 0.345 | 0.674 |
| *Camelus* | 0.183 | 0.231 | 0.322 | 0.676 | 0.197 | 0.249 | 0.347 | 0.729 | 0.190 | 0.240 | 0.335 | 0.702 |
| *Lama* | 0.280 | 0.443 | 0.481 | 0.992 | 0.181 | 0.285 | 0.310 | 0.640 | 0.231 | 0.364 | 0.396 | 0.816 |
| *Sus* | 0.189 | 0.238 | 0.339 | 0.606 | 0.143 | 0.180 | 0.257 | 0.458 | 0.166 | 0.209 | 0.298 | 0.532 |
| *Equus* | 0.286 | 0.388 | 0.545 | 0.886 | 0.150 | 0.203 | 0.286 | 0.464 | 0.218 | 0.295 | 0.415 | 0.675 |
| *Tapirus* | 0.283 | 0.416 | 0.595 | 1.179 | 0.229 | 0.336 | 0.481 | 0.952 | 0.256 | 0.376 | 0.538 | 0.813 |

more posteriorly directed vector because of the great development of the temporalis. In our sample, the dromedary has longer lever arms for the temporalis than for the masseter, in agreement with Greaves' (1991) ideas. The temporalis muscle mass in the tapir is greater than in the other herbivorous forms, and coincidently this animal has a long temporalis lever arm (although a little shorter than that of masseter). In this animal the principal chewing movement is orthal (Harris 1975), rather than the predominantly lateral movement seen in the other herbivorous forms mentioned.

In summary, the extension of the method of Vizcaíno et al. (1998) to the three-dimensional plane produces results that conform to what is known about the masticatory mechanics of the control sample taxa.

### Masticatory Biomechanics of Santacrucian Ungulates

All Santacrucian ungulates have a high condyle well above the occlusal plane (see Figs. 1, 5). Since the classical works (e.g., Maynard Smith and Savage 1959; Crompton and Hiiemae 1969), this feature has been known to characterize many herbivorous mammals and suggests improved leverage for certain masticatory muscles (i.e., masseter). However, with the exception of one genus (*Pachyrukhos*), all Santacrucian ungulates have a well-developed temporalis and masseter, with no evidence of better mechanical advantage for the latter, despite the high condyle (relative to the tooth row). This is in agreement with Greaves' (1974) postulate that condyle height and the masticatory moment arms can change independently of each other. In addition, a high condyle allows for simultaneous occlusion along the tooth row, provided that the glenoid fossa is equally high above the upper tooth row (Greaves 1980).

Among the notoungulates, *Adinotherium* and *Nesodon* (Nesodontinae) show the best mechanical advantage for an anterior bite point, whether considering the temporalis alone, or both masticatory muscles are considered together (Table 4). Surprisingly, the values are very similar to the ones observed in the puma, a specialized carnivore with a proportionately short rostrum. This should not be interpreted as an inference of carnivorous habits for nesodontines, but it increases the likelihood of such a behavioral hypothesis. Both *Adinotherium* and *Nesodon* have hypertrophied lateral incisors, and an unusually robust muzzle, which suggests potentially aggressive behaviors, in addition to obvious defensive uses.

It is also remarkable, that among notoungulates, only the hegetotheriid *Pachyrukhos* possesses the characteristic leverage ratio of extant herbivores, with the masseter having a better mechanical advantage than temporalis. All the remaining notoungulates fail to fit with the biomechanical model of specialized herbivory (grazer and browser) for extant ungulates. The configuration of the mandibular lever system of the nesodontines and interatheriids shows a predominance of mechanical advantage for the temporalis compared to the masseter. Furthermore, when both muscles are considered together, they present a mechanical configuration for postcanine bites that is similar to the case for the tapir. Leverage in nesodontines and interatheriids appears to enhance force all along the postcanine dental series, in a very similar way to what occurs in the tapir. Therefore, their masticatory apparatus was probably capable of producing proportionally strong bites along the dental series, particularly of the molars, which would allow them to process hard items, while enabling effective transverse chewing movements.

Among the Santacrucian litopterns, leverage of the masseter and the temporalis are in the range of the values obtained for camelids. The temporalis is large, as is evident from the great development of the sagittal crest and the origin areas, and has the same mechanical advantage as masseter, except at the posterior end of the molar tooth row where the masseter has more mechanical advantage. From a biomechanical point of view, and considering its larger body size, *Theosodon* has the most gracile masticatory system among Santacrucian litopterns. This suggests that among litopterns, the macraucheniids would feed on softer items than the proterotheriids. *Theosodon* has caniniform incisors. *Theosodon* must have had poor mechanical advantage at the anterior end of the muzzle, much like the case for the maned wolf; this could be an adaptation for chewing speed instead of force. Also, the incisors could have participated in food handling, as well as other functions.

*Astrapotherium* is another Santacrucian ungulate with a very particular morphology. The mechanical design of the masticatory apparatus, particularly in the anterior region of the jaw, is quite similar to that of the tapir, although more gracile. The mechanical advantages of the masseter and temporalis are very similar all along the jaw. Therefore, much as in litopterns (potentially), orthal and lateral masticatory movements were presumably equally important. At the anterior end of the jaw, their design favors speed over force, consistent with the wide diastema between the lower canine and first premolar. The jaw extends in front of the cranium, so that the lower incisors do not occlude with any bony or dental structure, suggesting that no powerful bite was possible here. In the posterior region of the molar tooth row there is a clear mechanical advantage (for force), similar to that in notoungulates (particularly nesodontines). In addition, *Astrapotherium* has proportionally the shortest postcanine tooth row of this fauna, due to the reduction in number and size of the premolars (Kramarz and Bond 2009). The areas of origin and insertion of the main masticatory muscles do not suggest the development of a great muscular mass for this taxon. Nevertheless, the capacity to maintain a mechanical advantage is assured through the proximity of the tooth row to the temporomandibular joint.

### Diet Considerations

Although, it has been proposed that the masticatory forces required to comminute grass are greater than for dicotyledons (Solounias and Dawson-Saunders 1988; Mendoza et al. 2002), they have been not yet tested and/or verified. Clauss et al. (2008: table 3.1) indicate that grasses are more resistant to grinding than dicotyledons. Regarding diet classifications, Cassini et al. (2011, in press) using ecomorphological and ontogenetic allometric approaches, respectively, concluded that nesodontines, particularly *Nesodon*, could not be characterized as specialist herbivores (grazer or browser), suggesting instead generalized herbivory. On the other hand, Townsend and Croft (2008), based on enamel microwear analyses, postulated browsing habits for *Protypotherium*, *Adinotherium*, and *Nesodon*. They concluded that the last could have had a diet richer in hard-objects (e.g., bark). According to Cassini et al. (2011) and Tauber (1996), typotheres were likely mainly open habitat grazers. Among Litopterna, proterotheriids have been characterized as browsers (Soria 2001; Villafañe et al. 2006). If the hypothesis mentioned above about the forces required to comminute grass and dicots is true, then greater muscle leverage in notoungulates compared to litopterns is consistent with grass consumption in the former and dicot feeding in the latter. In addition, the capabilities of nesodontines to achieve larger forces (among Santacrucian ungulates) give support to the more hard-object diet conclusions of Townsend and Croft (2008).

Another biomechanical aspect to be considered is the relationship with hypsodonty. Billet et al. (2009) described two hypotheses about the possible causes of the rise of hypsodonty within notoungulates. These are “an increase of abrasives consumed” and “an increasing chewing effort.” The second hypothesis, in particular, concerns the toughness of the plant, i.e., “a given particle size of food can be obtained by investing less chewing energy when eating fragile plants as compared to tougher species” (Pérez-Barbería and Gordon 1998: 246). Since notoungulates show a configuration that improves force capabilities of the masticatory apparatus as compared to litopterns, and, at the same time, notoungulate were hypsodont forms whereas litopterns were brachydont (see introduction), the increasing chewing effort hypothesis of Billet et al. (2009) seems to be consistent with our results. Only *Pachyrukhos*, which shows a similar mechanical configuration to extant ungulates (e.g., horse and huemul), contradicts the above reasoning, because it is the most hypsodont notoungulate in the sample (see Reguero et al. 2010) and at least as gracile as the litoptern *Theosodon*.

## Conclusions

Extending the geometric model developed by Vizcaíno et al. (1998) to a three-dimensional framework shows coherent results when an extant mammal test sample was analyzed.

The ungulates of the Santa Cruz Formation, with the exception of litopterns and *Pachyrukhos* (which resemble camels and cervids, respectively), fail to possess the typical herbivore mechanical configuration of the masticatory system with predominance of the masseter over the temporalis. The fact that the temporalis moment arms were as long as those of the masseter (or even longer in notoungulates) is consistent with the great development of the temporalis muscle as well as in with hypertrophied incisors (particularly nesodontines and proterotheriids).

When both muscles are considered together, notoungulates (except *Pachyrukhos*) have a better capability to develop force along the molar tooth row than do the litopterns. This indicates a diet rich in tough plant materials in notoungulates (e.g., grass or even bark) as compared to litopterns (e.g., dicots), which is consistent (in broad terms) with previous ecomorphological inferences. In addition, “an increasing chewing effort” hypothesis for hypsodonty in notoungulates sensu Billet et al. (2009) is partially supported.

Finally, the approach proposed here appears to be useful in comparing masticatory performance and is a powerful tool to validate ecomorphological diet hypotheses for fossil taxa.

**Acknowledgments** We thank the following persons and institutions. The Dirección de Patrimonio Cultural and Museo Regional Provincial Padre M. J. Molina (Río Gallegos, Santa Cruz Province) for allowing us to study material under their care. For access to vertebrate paleontological collection, we thank Dr. Marcelo Reguero from MLP, Dr. Alejandro Kramarz and Dr. Juan C. Fernicola from MACN, Dr. John Flynn from AMNH, Dr. Walter Joyce from YPM, and Dr. Itatí Olivares from Mastozoología-MLP; Lic. Nestor Toledo for the illustrations in Figure 3; Dr. Jonathan Perry for valuable suggestions that improved the manuscript and to the two anonymous reviewers that helped to enhance our work; Dr. Annat Haber for the R-functions and encouraging us to work with R. The study of the US/YPM collections was partially funded by the John H. Ostrom Research Fund to G. H. Cassini. This is a contribution to the Projects PICT 26219 and PICT 0143 of the Agencia Nacional de Promoción Científica y Tecnológica, PIP 1054 of the Consejo Nacional de Investigaciones Científicas y Técnicas, and N647 of the Universidad Nacional de La Plata to S.F. Vizcaíno, National Science Foundation to R.F. Kay, and National Geographic Society to S.F. Vizcaíno and R.F. Kay.

## Appendix 1

List of Santacrucian ungulate skulls examined in this work including taxonomic identification, mean body mass estimations from Cassini (2011) and collection numbers.

Notoungulata

Toxodontia (Toxodontidae): *Adinotherium* (105 kg) MACN-SC 4355; MPM-PV 3666 and MACN-A 5352–53. *Nesodon* (673 kg)YPM-PU 15000, 15256, 15336 and 15492.

Typotheria, Interatheriidae: *Interatherium* (2.51 kg) MPM-PV 3469, 3471, 3527; YPM-PU 15296 and 15401. *Protypotherium* (6.7 kg) AMNH 9482, 9565; YPM-PU 15828. Hegetotheriidae: *Pachyrukhos* (2.13 kg) AMNH 9283.

Litopterna

Proterotheriidae: *Diadiaphorus* (81 kg) AMNH 9291; MPM 3397; MACN-A 9200–9208 and 9180–82. *Tetramerorhinus* (35 kg) MACN-A 8970–71. Macraucheniidae: *Theosodon* (131 kg) MACN-A 2487–90 and 9269–88.

Astrapotheria

Astrapotheriidae: *Astrapotherium* (1124 kg) AMNH 9278 and YPM-PU 15332.

## Appendix 2

List of extant mammals skulls used in this work as reference sample including vernacular name, collection numbers, taxonomic identification, diet guild, body mass and observations.

*Chrysocyon brachyurus* “maned wolf” MLP 564: Carnivora (Canidae), carnivore feeding on small prey. *Puma concolor* “puma” MLP 1311: Carnivora (Felidae), carnivore feeding on big prey. *Camelus dromedarius* “dromedary” MLP 1622 and *Lama guanicoe* “guanaco” MLP 1367: Artiodactyla (Camelidae), mix-feeder herbivores of 415 kg and 130 kg respectively. *Hippocamelus bisulcus* “huemul” MLP 1364: Artiodactyla (Cervidae), browser herbivore of 85 kg. *Sus scrofa* “boar” MLP 20.III.02.5: Artiodactyla (Suidae), generalist omnivore of 86 kg. *Equus caballus* “horse” MLP 1547: Perissodactyla (Equidae), grazer herbivore of 350 kg. *Tapirus terrestris* “tapir” MLP 1681: Perissodactyla (Tapiridae), browser herbivore of 245 kg.

## References

Ameghino F (1887) Enumeración sistemática de las especies de mamíferos fósiles coleccionados por Carlos Ameghino en los terrenos eocenos de la Patagonia austral y depositados en el Museo La Plata. Bol Mus La Plata 1:1–26

Ameghino F (1889) Contribución al conocimiento de los mamíferos fósiles de la República Argentina. Actas Acad Nac Cien Córdoba 6:1–1027

Ameghino F (1894) Enumération synoptique des espèces de mammifères fossiles des formations éocènes de Patagonie. Bol Acad Cien Córdoba 13:259–452

Ameghino F (1898) Sinopsis geológico-paleontológica de la Argentina. Censo Nacional de la República Argentina, Tomo I (Territorio), Capítulo I, Parte 3. Buenos Aires, pp 113–255

Ameghino F (1907) Les toxodontes à cornes. An Mus Nac Hist Nat Buenos Aires 16:49–91

Aragona M, Setz EZF (2001) Diet of the maned wolf, *Chrysocyon brachyurus* (Mammalia: Canidae), during wet and dry seasons at Ibitipoca State Park, Brazil. J Zool (Lond) 254:131–136

Bargo MS (2003) Biomechanics and palaeobiology of the Xenarthra: the state of the art. Senckenberg Biol 83:41–50

Bargo MS, Vizcaíno SF (2008) Paleobiology of Pleistocene ground sloths (Xenarthra, Tardigrada): biomechanics, morphogeometry and ecomorphology applied to the masticatory apparatus. Ameghiniana 45:175–196

Billet G (2010) New observations on the skull of *Pyrotherium* (Pyrotheria, Mammalia) and new phylogenetic hypotheses on South American ungulates. J Mammal Evol 17:21–59

Billet G, Blondel C, Muizon C de (2009) Dental microwear analysis of notoungulates (Mammalia) from Salla (late Oligocene, Bolivia) and discussion on their precocious hypsodonty. Palaeogeogr Palaeoclimatol Palaeoecol 274:114–124

Bonaparte JF, Morales J (1997) Un primitivo Notonychopidae (Litopterna) del Paleoceno inferior de Punta Peligro, Chubut, Argentina. Estud Geol (Madr) 53:263–274

Bond M (1986) Los ungulados fósiles de Argentina: evolución y paleoambientes. Simposio “Evolución de los Vertebrados Cenozoicos” IV Congreso Argentino de Paleontologia y Bioestratigrafia Actas 2. Mendoza, 23–27 Noviembre, 1986, pp 187–190

Bond M (1999) Quaternary native ungulates of southern South America. A synthesis. In: Rabassa J, Salemme M (eds) Quaternary of South America and Antarctic Peninsula. Ushuaia, Tierra de Fuego: Centro Austral de Investigaciones Científicas and Universidad Nacional de la Patagonia, pp 177–205

Bond M, Cerdeño E, López G (1995) Los ungulados nativos de América del Sur. In: Alberdi MT, Leone G, Tonni EP (eds) Evolución biológica y climática de la región Pampeana durante los últimos cinco millones de años Un ensayo de correlación con el Mediterráneo occidental. Madrid: Monografías del MNCN, CSIC, pp 259–275

Bond M, García M (2002) Nuevos restos de toxodonte (Mamalia, Notoungulata) en estratos de la Formación Chucal, Mioceno, Altiplano de Arica, norte de Chile. Rev Geol Chile 29:81–91

Bond M, Perea D, Ubilla M, Tauber AA (2001) *Neolicaphrium recens* Frenguelli, 1921, the only surviving Proterotheriidae (Litopterna, Mammalia) into the South American Pleistocene. Palaeovertebrata 30:37–50

Bondesio P (1986) Lista sistemática de los vertebrados terrestres del Cenozoico de Argentina. Simposio “Evolución de los Vertebrados Cenozoicos” IV Congreso Argentino de Paleontologia y Bioestratigrafia Actas 2. Mendoza, 23–27 Noviembre, 1986, pp 187–190

Cassini GH (2011) Paleobiología de ungulados de la Formación Santa Cruz (Mioceno temprano-medio), Patagonia, Argentina. Una aproximación morfométrica y morfofuncional al estudio del aparato masticatorio. [Doctoral thesis]. Universidad Nacional de La Plata, La Plata, Buenos Aires, Argentina, 320 pp

Cassini GH, Flores DA, Vizcaíno SF (in press) Postnatal ontogenetic scaling of Nesodontine (Notoungulata, Toxodontidae) cranial morphology. Acta Zool (Stockh) doi:10.1111/j.1463-6395.2011.00501.x

Cassini GH, Mendoza M, Vizcaíno SF, Bargo MS (2011) Inferring habitat and feeding behaviour of early Miocene notoungulates from Patagonia. Lethaia 44:153–165

Christiansen P, Adolfssen JS (2005) Bite forces, canine strength and skull allometry in carnivores (Mammalia, Carnivora). J Zool (Lond) 266:133–151

Cifelli RL (1985) South American ungulate evolution and extinction. In: Stehli FG, Webb SD (eds) The Great American Biotic Interchange. Plenum Press, New York, pp 249–266

Cifelli RL (1993) The phylogeny of the native South American ungulates. In: Szalay FS, Novacek MJ, McKenna MC (eds) Mammals Phylogeny: Placentals. Springer-Verlag, New York and London, pp 195–216

Clauss M, Kaiser T, Hummel J (2008) The morphophysiological adaptations of browsing and grazing mammals. In: Gordon IJ, Prins HHT (eds) The Ecology of Browsing and Grazing. Springer-Verlag, Berlin Heidelberg, pp 47–88

Covey DSG, Greaves WS (1994) Jaw dimensions and torsion resistance duting canine biting in the Carnivora. Can J Zool 72:1055–1060

Croft DA (1999) Placentals: endemic South American ungulates. In: Singer R (ed) The Encyclopedia of Paleontology. Fitzroy-Dearborn, Chicago, pp 890–906

Crompton AW, Hiiemae K (1969) How mammalian molar teeth work. Discovery 5:23–34

De Iuliis G, Bargo MS, Vizcaíno SF (2000) Variation in skull morphology and mastication in the fossil giant armadillos *Pampatherium* spp. and allied genera (Mammalia: Xenarthra: Pampatheriidae), with comments on their systematics and distribution. J Vertebr Paleontol 20:743–754

Desojo JB, Vizcaíno SF (2009) Jaw biomechanics in the South American aetosaur *Neoaetosauroides engaeus*. Palaeontol Z 83:499–510

Duarte RE, Riestra JA (2004) Una justicación de la de noción de momento estático y de la correspondiente condición de equilibrio de un sólido. Misc Mat 40:29–52

Gabbert SL (2004) The basicranial and posterior cranial anatomy of the families of the Toxodontia. Bull Am Mus Nat Hist 285:177–190

Gelfo JN, López GM, Bond M (2008) A new Xenungulata (Mammalia) from the Paleocene of Patagonia, Argentina. J Paleontol 82:329–335

Greaves WS (1974) Functional implications of mammalian jaw joint position. Forma et Functio 7:363–376

Greaves WS (1980) The mammalian jaw mechanism. The high glenoid cavity. Am Nat 116:432–440

Greaves WS (1985) The generalized carnivore jaw. Zool J Linn Soc 85:267–274

Greaves WS (1988) The maximum average bite force for a given jaw length. J Zool 214:295–306

Greaves WS (1991) The orientation of the force of the jaw muscles and the length of the mandible in mammals. Zool J Linn Soc 102:367–374

Greaves WS (1995) Functional predictions from theoretical models of the skull and jaws in retiles and mammals. In: Thomason JJ (ed) Functional Morphology in Vertebrate Paleontology. Cambridge Universtity Press, Cambridge, pp 99–115

Harris JM (1975) Evolution of feeding mechanisms in the family Deinotheriidae (Mammalia: Proboscidea). Zool J Linn Soc 56:331–362

Hildebrand M (1988) Analysis of Vertebrate Structure. John Wiley & Sons, Inc, USA, 701 pp

Johnson SC, Madden RH (1997) Uruguaytheriine astrapotheres of tropical SouthAmerica. In: Kay RF, Madden RH, Cifelli RL, Flynn JJ (eds) Vertebrate Paleontology in the Neotropics: The Miocene Fauna of La Venta, Colombia. Smithsonian Institution Press, Washington, DC, pp 355–381

Kramarz AG (2009) Adiciones al conocimiento de *Astrapothericulus* (Mammalia, Astrapotheria): anatomía cráneo-dentaria, diversidad y distribución. Rev Bras Biol 12:55–66

Kramarz AG, Bond M (2009) A new Oligocene astrapothere (Mammalia, Meridiungulata) from Patagonia and a new appraisal of astrapothere phylogeny. J Syst Palaeontol 7:117–128

Marshall LG, Cifelli RL (1989) Analysis of. changing diversity patterns in Cenozoic. Land mammal age faunas, South America. Paleovertebrata 19: 169–210

Marshall LG, Salinas P, Manuel S (1990) *Astrapotherium* sp. (Mammalia Astrapotheriidae) from Miocene strata along the Quepuca river, central Chile. Rev Geol Chile 17:215–223

Martin PS, Steadman DW (1999) Prehistoric extinctions on islands and continents. In: MacPhee RDE (ed) Extinctions in Near Time: Causes, Contexts and Consequences. Kluwer/Plenum, New York, pp 17–56

Maynard Smith J, Savage RJG (1959) The mechanics of mammalian jaws. Sch Sci Rev 141:289–301

McKenna MC (1975) Toward a phylogenetic classification of mammals. In: Lucket WP, Szalay FS (eds) Phylogeny of the Primates. Plenum, New York, pp 21–46

Mendoza M, Janis CM, Palmqvist P (2002) Characterizing complex craniodental patterns related to feeding behaviour in ungulates: a multivariate approach. J Zool 258:223–246

Mones A (1982) An equivocal nomenclature: what means hypsodonty? Palaeontol Z 56:107–111

Muizon C de, Cifelli RL (2000) The “condylarths” (archaic Ungulata, Mammalia) from the early Palaeocene of Tiupampa (Bolivia): implications on the origin of the South American ungulates. Geodiversitas 22:47–150

Owen-Smith N (1988) Megaherbivores. The Influence of Very Large Body Size on Ecology. Cambridge: Cambridge University Press.

Pascual R, Ortiz-Jaureguizar E, Prado JL (1996) Land mammals: paradigm for Cenozoic South American geobiotic evolution. In: Arratia G (ed) Contribution of Southern South America to Vertebrate Paleontology. Geowissenshaftliche Abhandlungen, München, pp 265–319

Patterson B, Pascual R (1968) The fossil mammal fauna of South America. Q Rev Biol 43:409–451

Patterson B, Pascual R (1972) The fossil mammal fauna of South America. In: Keast A, Erk FC, Glass B (eds) Evolution, Mammals, and Southern Continents. University of New York State Press, Albany, pp 247–309

Pérez-Barbería FJ, Gordon IJ (1998) Factors affecting food comminution during mastication in herbivorous mammals: a review. Biol J Linn Soc 63:233–256

Radinsky, LB (1981) Evolution of skull shape in carnivores. 1. Representative modern carnivores. Biol J Linn Soc 15:369–388.

Reddy DP, Kim J, Raaum R (2007) Resample.exe: http://pages.nycep.org/nmg/programs.html.

Reguero MA, Candela AM, Cassini GH (2010) Hypsodonty and body size in rodent-like notoungulates. In: Madden RH, Carlini AA, Vucetich MG, Kay RF (eds) The Paleontology of Gran Barranca: Evolution and Environmental Change through the Middle Cenozoic of Patagonia. Cambridge University Press, Cambridge, pp 362–371

Reguero MA, Dozo MT, Cerdeño E (2007) A poorly known rodentlike mammal (Pachyrukhinae, Hegetotheriidae, Notoungulata) from the Deseadan (late Oligocene) of Argentina. Paleoecology, biogeography, and radiation of the rodentlike ungulates in South America. J Paleontol 81:1301–1307

Rensberger JM, Pfretzschner HU (1992) Enamel structure in astrapotheres and its functional implications. Scann Microsc 6:495–510

Riggs ES (1935) A skeleton of *Astrapotherium*. Fieldiana Geol 6:167–177

Scott WB (1912) Mammalia of the Santa Cruz beds. Part II. Toxodonta. Part III. Entelonychia. In: Scott WB (ed) Reports of the Princeton University Expeditions to Patagonia, 1896–1899. Princeton University, Princeton, pp 111–300

Scott WB (1913) A History of Land Mammals in the Western Hemisphere. The MacMillan Company, New York, 732 pp

Scott WB (1928) Mammalia of the Santa Cruz beds. Part IV. Astrapotheria. In: Scott WB (ed) Reports of the Princeton University Expeditions to Patagonia, 1896–1899. Princeton University, Princeton, pp 301–352

Scott WB (1937) The Astrapotheria. Proc Am Phil Soc 77:309–393

Schaller O (2007) Illustrated Veterenary Anatomical Nomenclature. Enke Verlag, Stuttgart, 614 pp

Shockey BJ, Croft DA, Anaya F (2007) Analysis of function in the absence of extant functional homologues: a case study using mesotheriid notoungulates (Mammalia). Paleobiology 33:227–247

Simpson GG (1936) Structure of a primitive notoungulate cranium. Am Mus Novitates 824:1–31

Simpson GG (1950) History of the fauna of Latin America. Sci Am 38:361–389

Simpson GG (1967) The beginning of the age of mammals in South America. Part II. Bull Am Mus Nat Hist 137:1–260

Simpson GG (1980) Splendid Isolation: the Curious History of South American Mammals. Yale University Press, New Haven, 274 pp

Sinclair WJ (1909) Mammalia of the Santa Cruz beds. Part I. Typotheria. In: Scott WB (ed) Reports of the Princeton University Expeditions to Patagonia, 1896–1899. Princeton University, Princeton, pp 1–110

Solounias N, Dawson-Saunders B (1988) Dietary adaptations and palaecology of the late Miocene ruminants from Pikermi and Samos in Greece. Palaeogeogr Palaeoclimatol Palaeoecol 65:149–172

Soria MF (2001) Los Proterotheriidae (Litopterna, Mammalia), sitemática, origen y filogenia. Monogr Mus Argentino Cienc Nat 1:1–167

Soria MF, Powell JE (1981) Un primitivo Astrapotheria (Mammalia) y la Edad de la Formación Río Loro, provincia de Tucumán, República Argentina. Ameghiniana 18:155–168

Tauber AA (1996) Los representantes del género *Protypotherium* (Mammalia, Notoungulata, Interatheridae) del Mioceno Temprano del sudoeste de la Provincia de Santa Cruz, República Argentina. Academia Nacional de Ciencias, Córdoba, Miscelanea pp 3–29

Townsend KEB, Croft DA (2008) Diets of notoungulates from the Santa Cruz Formation, Argentina: new evidence from enamel microwear. J Vertebr Paleontol 28:217–230

Turnbull WD (1970) Mammalian masticatory apparatus. Fieldiana Geol 18:1–356

Villafañe AL, Ortiz-Jaureguizar E, Bond M (2006) Cambios en la riqueza taxonómica y en las tasas de primera y última aparición de los Proterotheriidae (Mammalia, Litopterna) durante el Cenozoico. Estud Geol 62:155–166

Vizcaíno SF, Bargo MS (1998) The masticatory apparatus of the armadillo *Eutatus* (Mammalia, Cingulata) and some allied genera: paleobiology and evolution. Paleobiology 24:371-383

Vizcaíno SF, Bargo MS, Kay RF, Milne N (2006) The armadillos (Mammalia, Xenarthra, Dasypodidae) of the Santa Cruz Formation (early-middle Miocene): an approach to their paleobiology. Palaeogeogr Palaeoclimatol Palaeoecol 237:255-269

Vizcaíno SF, De Iuliis G (2003) Evidence for advanced carnivory in fossil armadillos. Paleobiology 29:123-138

Vizcaíno SF, De Iuliis G, Bargo MS (1998) Skull shape, masticatory apparatus, and diet of *Vassallia* and *Holmesina* (Mammalia: Xenarthra: Pampatheriidae). When anatomy constrains destiny. J Mammal Evol 5:291-322

Westneat MW (2003) A biomechanical model for analysis of muscle force, power output and lower jaw motion in fishes. J Theor Biol 223:269–281

Witmer LM (1995) The Extant Phylogenetic Bracket and the importance of reconstructing soft tissues in fossils. In: Thomason JJ (ed) Functional Morphology in Vertebrate Paleontology. Cambridge University Press, Cambridge, pp 19-33